BeBeC-2018-D08

Comparison of different solvers for general inverse beamforming algorithms for highresolution aeroacoustic source characterization

Simon Jekosch[1],Ennes Sarradj[1], Gert Herold[1] and Thomas Geyer[2]
[1]Technische Universität Berlin
Einsteinufer 25, 10587 Berlin, Germany
[2]Brandenburg University of Technology
Siemens-Halske-Ring 14, 03046 Cottbus, Germany

Abstract

Identification of acoustic sources plays an important role in acoustic design improvements for a wide area of applications. Eigenvalue based general inverse beamforming (GIB) has proven to be a valuable tool for acoustic source characterization. This work aims to compare different regularization strategies which solve the GIB algorithm. The classical L_1 formulation of GIB is compared with LassoLars, Orthogonal Matching Pursuit and non-negative least squares solvers. The algorithms are applied to measured data from an airfoil in an open jet with a planar microphone array. The NACA-0012 airfoil under subsonic flow conditions is described using monopole identifications. The GIB results are compared qualitatively and quantitatively to previous beamforming results using DAMAS and CMF algorithms.

1 INTRODUCTION

Noise source identification by source map imaging using phased microphone arrays has become a useful and common tool in acoustic engineering. Aside from classic delay-and-sum (DAS) beamforming, several deconvolution algorithms have been developed and tested to increase the resolution of the beamforming result. Acoustic studies on a reference setup on an airfoil have been conducted by Herold et al.[5, 6] using DAMAS[2], CMF[17], CLEAN-SC[14] and Orthogonal Beamforming[11] deconvolutions. Another representative algorithm is the generalized inverse beamforming (GIB) presented by Takao Suzuki [15]. The algorithm is based on the decomposition of the cross spectral matrix into eigenmodes and formulating a source model

for each eigenmode. The target of this contribution is to discuss GIB regularisation strategies, which are applied to measurement data of an airfoil in an open jet.

2 GENERAL INVERSE BEAMFORMING AND SOLVING STRATEGIES

Microphone array methods rely on the evaluation of signals recorded at a number of distributed sensors. The general inverse beamforming algorithm works in the frequency domain and is based on the calculation of the cross spectral matrix (**CSM**). For the signals of M microphones in an array the **CSM** can be computed using Welch's method [16]: The time signals from each microphone are divided into K blocks, onto which an FFT is applied, resulting in a complex pressure vector $\mathbf{p}_k$ for each discrete frequency. The **CSM** is calculated by averaging the cross spectra between the microphone channels:

$$\mathbf{CSM} = \frac{1}{K}\sum_{k=1}^{K}\mathbf{p}_k\mathbf{p}_k^H \tag{1}$$

Since the cross spectral matrix is Hermitian and non-negative definite, it can be decomposed into a unitary matrix $\mathbf{U}$ consisting the eigenvectors $\mathbf{u}_i$ and a diagonal matrix Λ consisting the corresponding eigenvalues λ_i:

$$\mathbf{CSM} = \mathbf{U}\Lambda\mathbf{U}^H \tag{2}$$

For each eigenvalue λ_i and eigenvector $\mathbf{u}_i$ we can define the an eigenmode $\mathbf{v_i}$ as:

$$\mathbf{v}_i = \sqrt{\lambda_i}\mathbf{u}_i \tag{3}$$

Each eigenmode can be related to a complex source amplitude $\mathbf{q}_i$ for each grid point N on a target domain. With a transfer matrix A we can define a linear system for each eigenmode:

$$\mathbf{v_i} = \mathbf{A}\mathbf{q}_i \tag{4}$$

For the source model monopole sources are considered. The entries of the transfer matrix A are calculated with :

$$A_{mn} = \frac{r_{0n}}{r_{mn}}e^{-ik(r_{mn}-r_{0n})}\ ,\ m\ =\ 1...M\ ,\ n\ =\ 1...N \tag{5}$$

with r_{0n} being the distance from one focus point to the m-th of M microphones and r_{mn} the distance from the m-th microphone to the n-th grid point. The system can be solved by minimizing the J_p cost function:

$$\text{minimize}\quad J_p = \|\mathbf{q}\|_p^p + \lambda(\mathbf{A}\mathbf{q}-\mathbf{v}_i) \tag{6}$$

which can be rewritten as:

$$\text{minimize}\quad J_p = \|\mathbf{W}\mathbf{q}\|_2^2 + \lambda(\mathbf{A}\mathbf{q}-\mathbf{v}_i) \tag{7}$$

The weight matrix $\mathbf{W}$ is a diagonal matrix, each element is given by $\mathbf{W}_{ii} = |q_i|^{p-2}$. The solution can be calculated iteratively using the generalized inverse technique as proposed by Suzuki

[15]. Depending on the size of the problem two different solutions exist. For an underdetermined system $(N > M)$ the system is solved by:

$$\hat{\mathbf{q}}^{it+1} = \mathbf{W}^{it}\mathbf{A}^H(\mathbf{A}\mathbf{W}^{it}\mathbf{A}^H + \varepsilon\mathbf{I})^{-1}\mathbf{v}_i) \tag{8}$$

For the overdetermined system $(N < M)$ it is solved by:

$$\hat{\mathbf{q}}^{it+1} = \mathbf{A}^H(\mathbf{A}\mathbf{A}^H + \varepsilon(\mathbf{W}^{it})^{-1})^{-1}\mathbf{v}_i) \tag{9}$$

With ε being a fraction of the biggest eigenvalue of $\mathbf{A}\mathbf{A}^H$. Alternatively to solving the complex valued system an equivalent real valued problem can be formulated [3]:

$$\begin{pmatrix} \Re\{\mathbf{A}\} & -\Im\{\mathbf{A}\} \\ \Im\{\mathbf{A}\} & \Re\{\mathbf{A}\} \end{pmatrix} \begin{pmatrix} \Re\{\mathbf{q}_i\} \\ \Im\{\mathbf{q}_i\} \end{pmatrix} = \begin{pmatrix} \Re\{\mathbf{v}_i\} \\ \Im\{\mathbf{v}_i\} \end{pmatrix} \tag{10}$$

The real valued problem can be rewritten as:

$$\overline{\mathbf{A}}\,\overline{\mathbf{q_i}} = \overline{\mathbf{v_i}} \tag{11}$$

The system can also be formulated such that it can be evaluated with efficient non-negative least squares (NNLS) solvers [7]:

$$\text{minimize} \quad \|\overline{\mathbf{v_i}} - \overline{\mathbf{A}}\,\overline{\mathbf{q}_i}\|_2 \quad , \quad \overline{\mathbf{q}_i} > 0 \tag{12}$$

The NNLS formulation can be extended with the introduction of a penalty term $\alpha\|\overline{\mathbf{q}_i}\|_1$

$$\text{minimize} \quad \|\overline{\mathbf{v_i}} - \overline{\mathbf{A}}\,\overline{\mathbf{q}_i}\|_2 + \alpha\|\overline{\mathbf{q}_i}\|_1 \quad , \quad \alpha > 0 \tag{13}$$

The combination of the regularisation factor α and the L_1 norm of the distributed source amplitudes enforces sparsity of the solution. By increasing α the penalty term increases and the sparsity of the solution increases as well. One possibility to solve this problem is using a Least Angle Regression Lasso algorithm (LassoLars) [4]. Choosing an optimal regularisation factor α for the algorithm depends on the measurement data and the experimental setup. There are different practical approaches to determine an optimal α. For example automatic criterion models like the Bayesian information criterion (BIC)[18] or eigenvalue based calculations like proposed by Yardibi [17]. Another possible algorithm for finding a sparse solution is the Orthogonal Matching Pursuit (OMP)[8, 9]. The principle of this greedy algorithm is to only use a subset of the available data, which is determined by iteratively selecting those columns of A which best approximate the eigenmode result v_i. For reducing possible reconstruction errors, a version of the algorithm employing cross-validation is used (OMPCV)[1].

For the evaluations in this study, the implementation of the above algorithms in the machine learning python library scikit-learn [10] were used in combination with the array data processing library Acoular [13].

3 EXPERIMENTAL SETUP

The experiment was conducted in an aeroacoustic wind tunnel at Brandenburg University of Technology [12]. The setup consists of a NACA 0012 airfoil positioned in an open jet (diameter

0.2 m, core velocity 50 $\frac{m}{s}$). The airfoil has a span of 0.28 m and a chord length of 0.25 m; boundary layer tripping was realized with a 2.5 mm anti-slip tape applied at 10% of the chord on the suction as well as on the pressure side. Figure 1 shows a schematic depiction of the measurement setup. The microphone array is positioned outside the flow and 0.715 m above the airfoil. It consists of 56 microphones and has a maximum diameter of 1.3 m. The measurement time was 40 s, with a sampling rate of 51 200 Hz. For the estimation of the cross spectral matrix, the time histories were partitioned into 1000 blocks of 4096 samples each. A Hanning window was applied to each block and an FFT and subsequent power spectrum average with 50% block overlap were used.

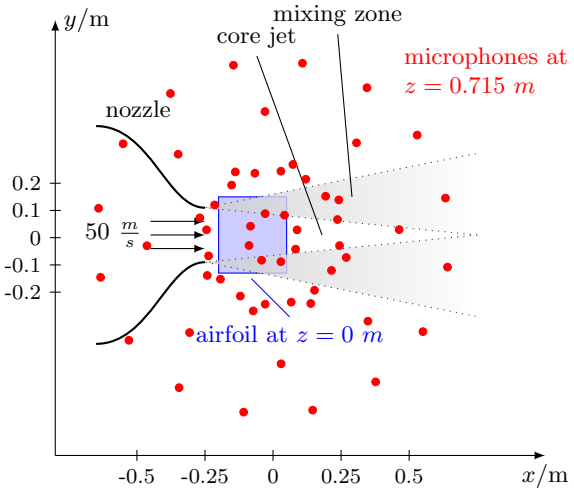

Figure 1: Setup used for the measurements.

4 RESULTS

Basis of the evaluations are sound pressure level maps for the 1/3 octave bands at 1, 2, 4, and 8 kHz, as shown in Figures 2 to 8. The nozzle is positioned at the left, and the position of the airfoil is marked by the blue rectangle in the center of the maps. The dotted lines indicate the integration areas for the trailing edge spectra shown in Figure 9.

The results of the general inverse beamforming algorithm strongly depend on the numbers of eigenvalues considered for the calculation. For this experimental setup, only the first 4 of 56 eigenvalues of the CSM contributed a significant amount to the result. Therefore, only the results for those 4 eigenvalues are considered in the calculation and displayed in the source maps.

The Figure 2 shows the result obtained with the general inverse beamforming algorithm of Suzuki. For the calculation the considered norm was set to L_1, the number of iterations to 10 and the regularisation parameter ε to 10^{-3}. At the 4 and 8 kHz bands the approach shows the trailing edge noise as a line source and the noise generation at the leading edge over the edges of the profile. For the 1 kHz band the noise generation at the nozzle and on the edges of the

trailing edge are visible. At 2 kHz the source identification does not show any airfoil noise and the highest values are reached at the border of the calculation area.

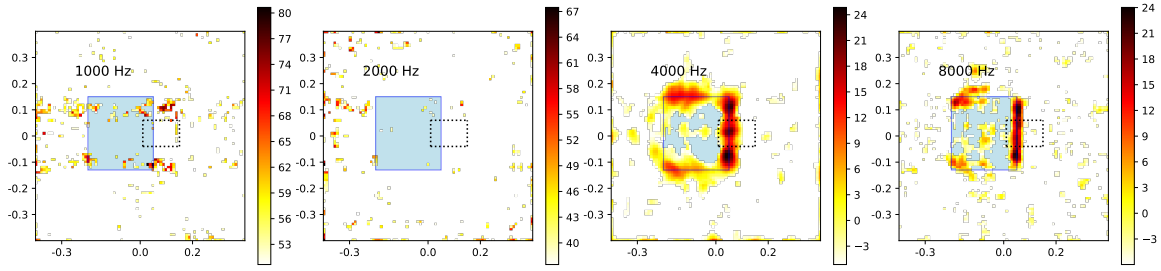

Figure 2: Source maps for the 1,2,4 and 8 kHz one-third octave bands, obtained with the GIB algorithm of Suzuki. The colorbars represent the sound pressure level L_p in dB.

The maps shown in Figure 3 is obtained using the NNLS solver [7] on Eq. 12. At the two lower frequency bands the solution is very sparse, but fails to identify the main sources. For the 2 higher frequency bands the identification is better, but the dynamic is very low and the solution contains artefacts.

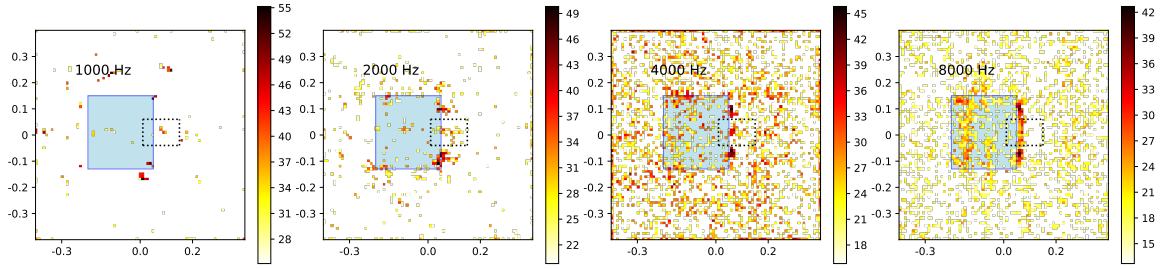

Figure 3: Source maps for the 1,2,4 and 8 kHz one-third octave bands, obtained with the GIB algorithm and NNLS solver.

The Figures 4 till 7 show maps using different α to solve Eq. 13 with a LassoLars solver [4]. For $\alpha = 10^{-4}$ the solution is reduced to a sound pressure of zero for the 2, 4 and 8 kHz band. For the 1 kHz band it is reduced to a small source at the trailing edge region. The regularisation parameter α is chosen too high in this case and the sparsity constraint is to strong to accomplish a suitable solution. Reducing α leads to more distributed noise sources, but reduces the possibility of resulting in a zero solution. Figure 5 shows the source maps obtained with $\alpha = 10^{-6}$. The noise sources at the trailing and leading edge become visible for all 4 one-third octave bands. The trailing edge noise appears as a line source at the 4 and 8 kHz bands. The maps for $\alpha = 10^{-9}$ are shown in Figure 6. The source distribution is very similar to the one with $\alpha = 10^{-6}$ but more detailed at the leading edge and not as sharp at the trailing edge, especially at 4 and 8 kHz bands. The lower regularisation factor leads also to a lower dynamic at higher frequencies. Decreasing α further would create a result similar to the NNLS result. Using an automatic algorithm to determine the optimal regularisation parameter can be

helpful for the calculation, since the manual selection of a suitable choice can be effortful. The BIC [18] is one possible method for the parameter selection of α. Figure 7 shows the source maps for the automatic calculated α according to the BIC. The criterion results in an α similar to $\alpha = 10^{-4}$. The solution is very sparse, with only a few non-zero points at the trailing and leading edge for the 1,2 and 4 kHz bands. For the solution for the 8 kHz band is all-zero.

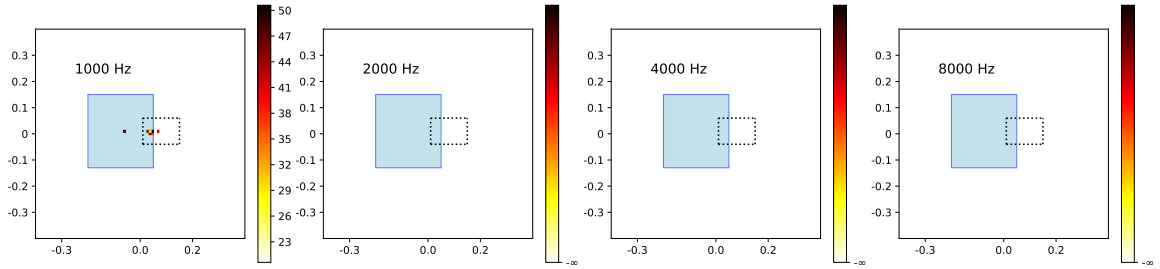

Figure 4: Source maps for the 1,2,4 and 8 kHz one-third octave bands, obtained with the GIB algorithm and LarsLasso solver with $\alpha = 10^{-4}$.

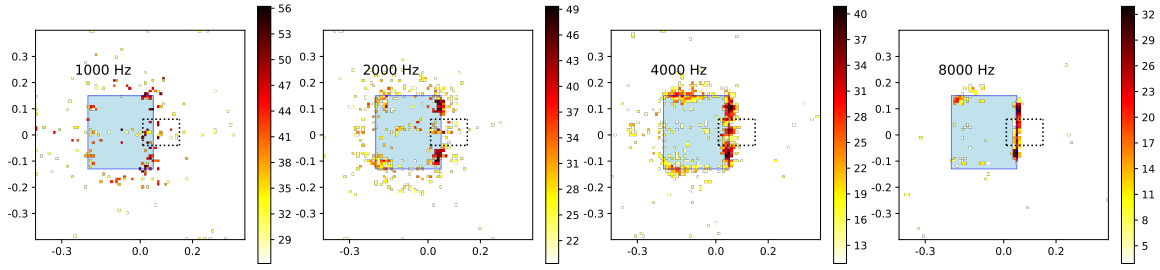

Figure 5: Source maps for the 1,2,4 and 8 kHz one-third octave bands, obtained with the GIB algorithm and LarsLasso solver with $\alpha = 10^{-6}$.

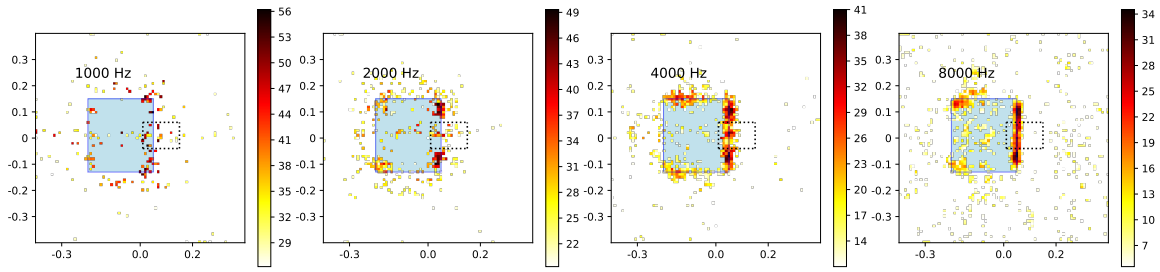

Figure 6: Source maps for the 1,2,4 and 8 kHz one-third octave bands, obtained with the GIB algorithm and LarsLasso solver with $\alpha = 10^{-9}$.

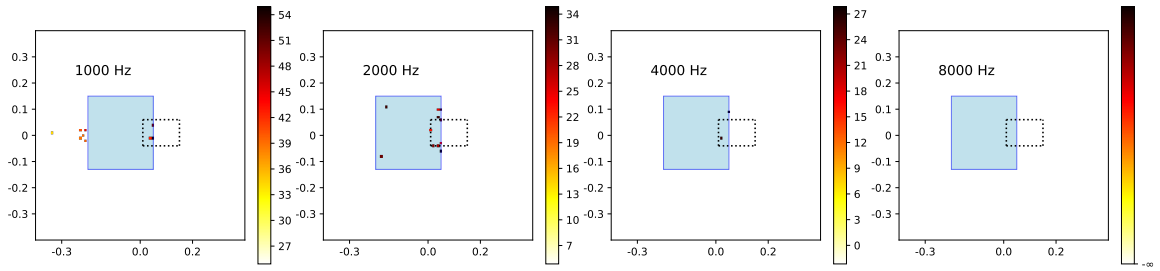

Figure 7: Source maps for the 1,2,4 and 8 kHz one-third octave bands, obtained with the GIB algorithm and LarsLasso solver with α chosen according to the BIC.

Figure 8 shows the result using the orthogonal matching pursuit method. The 1/3 octave bands at 4 and 8 kHz show a distribution like the LassLars solver with $\alpha = 10^{-6}$.However, the Trailing edge line source appears to by sharper at 8 kHz. At the 2 kHz band the leading and trailing edge sources are scattered over the airfoil area. The sources at the 1 kHz band are not distributed in a meaningful manner.

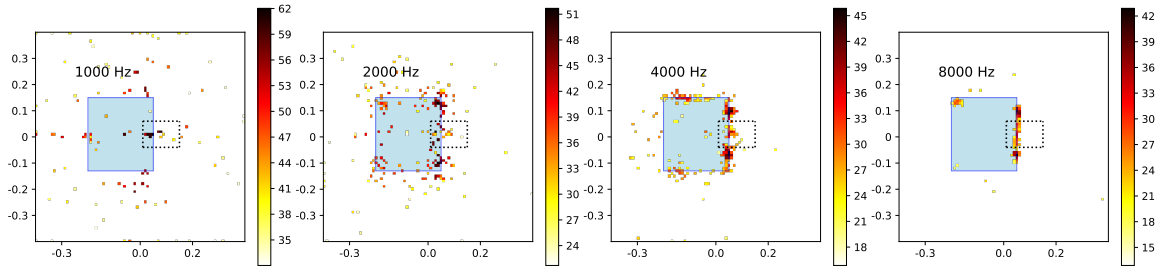

Figure 8: Source maps for the 1,2,4 and 8 kHz one-third octave bands, obtained with the GIB algorithm and OMPCV solver.

For quantitative comparison, the trailing edge spectra is computed by integrating the sound pressure over the area inside the dotted rectangle in the source maps. Figure 9 shows the one-third octave spectra for the different solvers between 800 and 10000 Hz. For a better distinction each line was shifted slightly, still the bands are centred around the frequencies on the x-axis. The spectra for the LassoLars solvers with $\alpha = 10^{-6}$ and $\alpha = 10^{-9}$ are almost identical to each other. The spectra for $\alpha = 10^{-4}$ and BIC strongly derivative from the others. This can be linked to the computation resulting in an all-zero solution for a wide range of frequencies. The OMPCV algorithm produces a spectrum with the same characteristics as the LassoLars with $\alpha = 10^{-6}$, but causes a approximately 10 dB higher sound pressure level. In contrast, the spectrum generated with the algorithm of Suzuki yields a lower sound pressure level. The spectrum produced by the NNLS solver also deviates heavily from the other spectra. Its maximum of 92.5 dB is reached at the 3.15 kHz band, which is not observable for any other algorithm.

Apart from the differences in the calculated source maps and spectra, the methods also differ in computational cost. The computation time for the generalized inverse beamforming is compared to the DAMAS and CMF using the same algorithms and parameters for each method.

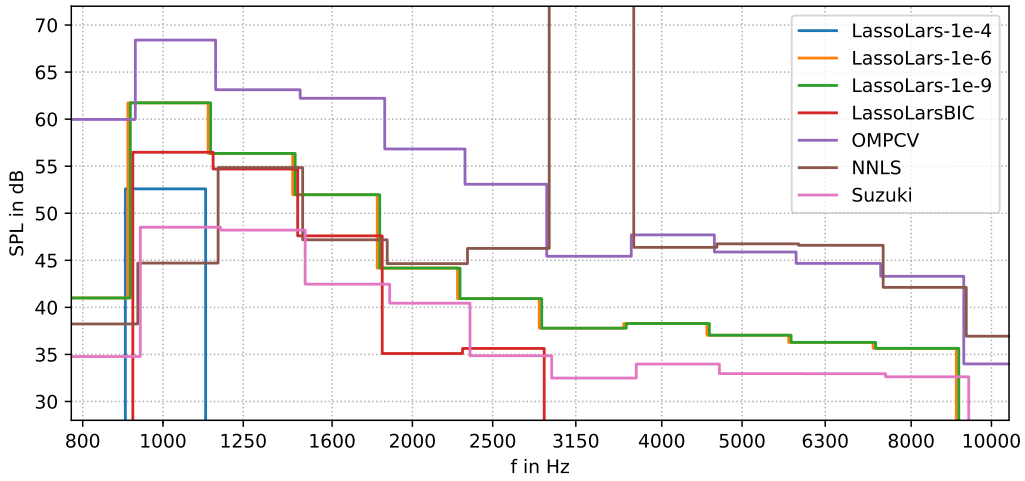

Figure 9: One-third octave spectra of trailing edge noise for different GIB algorithm solvers.

In Table 1 the relative calculation times are listed. The GIB-NNLS computation time is used as the comparative value. The calculation time for the point spread function, which is needed for the DAMAS calculation, is omitted in this comparison. The NNLS solver takes nearly the same time to solve the GIB and DAMAS method, but takes 5 times longer for the CMF method. The LassoLars algorithm is generally faster then NNLS, but takes longer for smaller α. For big enough α the calculation results in a all-zero solution very fast. The LassoLars-BIC algorithm is 40 times faster for the GIB method, but does not produce a meaningful result in this setup. The orthogonal matching pursuit takes the same order of computation time as NNLS for the GIB and CMF method, thought it takes about 4 times longer for the DAMAS deconvolution. The algorithm of Suzuki is considerable slower then the other algorithms in this study. However, this might also be an issue caused by a different implementation strategy.

Table 1: Relative calculation time for GIB, DAMAS and CMF.

	GIB	DAMAS	CMF
NNLS	1	0.82	5.42
LassoLars $\alpha = 10^{-4}$	0.23	0.14	0.30
LassoLars $\alpha = 10^{-6}$	0.31	0.13	0.29
LassoLars $\alpha = 10^{-9}$	0.63	0.27	2.05
LassoLarsBIC	0.25	-	9.79
OMPCV	1.28	3.53	5.42
Suzuki	21.19	-	-

5 Conclusion

The general inverse beamforming method was used on aeroacoustic measurement data from a wind tunnel experiment. Several different algorithms were used to solve the inverse problem. The results vary significantly based on the algorithm as well as on the parameters used for each algorithm. For this setup neither NNLS nor LassoLars with BIC and $\alpha = 10^{-4}$ as regularisation parameter provide a satisfying result. The method of Suzuki and OMP deliver good results above 4 kHz but fail to produce meaningful results at lower frequencies. The best overall performance was archived with the LassoLars algorithm and a fixed regularisation parameter.

REFERENCES

[1] P. Boufounos, M. F. Duarte, and R. G. Baraniuk. "Sparse Signal Reconstruction from Noisy Compressive Measurements using Cross Validation." *Statistical Signal Processing, 2007. SSP '07. IEEE/SP 14th Workshop on*, pages 299–303, 2007. doi:10.1109/SSP.2007.4301267.

[2] T. F. Brooks and W. M. Humphreys Jr. "A deconvolution approach for the mapping of acoustic sources (DAMAS) determined from phased microphone array." *J. Sound Vib.*, 294(4-5), 856–879, 2006. doi:10.1016/j.jsv.2005.12.046.

[3] D. Day and M. A. Heroux. "Solving complex-valued linear systems via equivalent real formulations." *SIAM Journal on Scientific Computing*, 23(2), 480–498, 2001. ISSN 1064-8275. doi:10.1137/s1064827500372262.

[4] B. Efron and T. Hastie. "Least angle regression." *The Annals of statistics*, 32(2), 407–499, 2004. ISSN 1095-9572. doi:10.1214/009053604000000067.

[5] G. Herold, T. Geyer, and E. Sarradj. "Comparison of inverse deconvolution algorithms for high-resolution aeroacoustic source characterization." *23rd AIAA/CEAS Aeroacoustics Conference, 2017*, pages 1–8, 2017.

[6] G. Herold, E. Sarradj, and T. Geyer. "Covariance Matrix Fitting for Aeroacoustic Application." In *Fortschritte der Akustik - DAGA*. 2013.

[7] C. L. Lawson. *Solving least squares problems /*. SIAM, Philadelphia, Pa. :, unabridged, rev. republ. (of the 1974 ed.) edition, 1995. ISBN 0-89871-356-0.

[8] S. Mallat and Zhifeng Zhang. "Matching pursuits with time-frequency dictionaries." *IEEE Transactions on Signal Processing*, 41(12), 3397–3415, 1993. ISSN 1053587X. doi:10.1109/78.258082.

[9] T. Padois and A. Berry. "Orthogonal matching pursuit applied to the deconvolution approach for the mapping of acoustic sources inverse problem." *The Journal of the Acoustical Society of America*, 138(6), 3678–3685, 2015. doi:10.1121/1.4937609.

[10] F. Pedregosa, G. Varoquaux, A. Gramfort, V. Michel, B. Thirion, O. Grisel, M. Blondel, P. Prettenhofer, R. Weiss, V. Dubourg, J. Vanderplas, A. Passos, D. Cournapeau, M. Brucher, M. Perrot, and E. Duchesnay. "Scikit-learn: Machine learning in Python." *Journal of Machine Learning Research*, 12, 2825–2830, 2011.

[11] E. Sarradj. "A fast signal subspace approach for the determination of absolute levels from phased microphone array measurements." *Journal of Sound and Vibration*, 329(9), 1553–1569, 2010. ISSN 0022460X. doi:10.1016/j.jsv.2009.11.009.

[12] E. Sarradj, C. Fritzsche, T. Geyer, and J. Giesler. "Acoustic and aerodynamic design and characterization of a small-scale aeroacoustic wind tunnel." *Applied Acoustics*, 70(8), 1073–1080, 2009. ISSN 0003682X. doi:10.1016/j.apacoust.2009.02.009.

[13] E. Sarradj and G. Herold. "A Python framework for microphone array data processing." *Applied Acoustics*, 116, 50–58, 2017. ISSN 1872910X. doi:10.1016/j.apacoust.2016.09.015.

[14] P. Sijtsma. "CLEAN based on spatial source coherence." *International Journal of Aeroacoustics*, 6, 357–374, 2007. doi:10.1260/147547207783359459.

[15] T. Suzuki. "L1 generalized inverse beam-forming algorithm resolving coherent/incoherent, distributed and multipole sources." *Journal of Sound and Vibration*, 330, 5835–5851, 2011. doi:10.1016/j.jsv.2011.05.021.

[16] P. D. Welch. "The Use of Fast Fourier Transform for the Estimation of Power Spectra: A Method Based on Time Averaging Over Short, Modified Periodograms." *IEEE Transactions on Audio and Electroacoustics*, 15(2), 70–73, 1967. ISSN 00189278. doi:10.1109/TAU.1967.1161901.

[17] T. Yardibi, J. Li, P. Stoica, and L. N. Cattafesta. "Sparsity constrained deconvolution approaches for acoustic source mapping." *The Journal of the Acoustical Society of America*, 123(5), 2631–2642, 2008. ISSN 00014966. doi:10.1121/1.2896754.

[18] H. Zou, T. Hastie, and R. Tibshirani. "On the "degrees of freedom" of the lasso." *Annals of Statistics*, 35(5), 2173–2192, 2007. ISSN 00905364. doi:10.1214/009053607000000127.